

Characteristics of Asperity Damage and Its Influence on the Shear Behavior of Granite Joints

Fanzhen Meng^{1,2} · Hui Zhou² · Zaiquan Wang¹ · Chuanqing Zhang² · Shaojun Li² · Liming Zhang¹ · Liang Kong¹

Received: 29 April 2017 / Accepted: 1 September 2017 / Published online: 26 September 2017
© Springer-Verlag GmbH Austria 2017

Abstract Surface roughness significantly affects the shear behavior of rock joints; thus, studies on the asperity damage characteristics and its influence on the shear behavior of joints are extremely important. In this paper, shear tests were conducted on tensile granite joints; asperity damage was evaluated based on acoustic emission (AE) events; and the influence of asperity damage on joint shear behavior was analyzed. The results indicated that the total AE events tended to increase with normal stress. In addition, the *asperity damage initiation shear stress*, which is defined as the transition point from slow growth to rapid growth in the cumulative events curve, was approximately 0.485 of the peak shear strength regardless of the normal stress. Moreover, 63–85% of the AE events were generated after the peak shear stress, indicating that most of the damage occurred in this stage. Both the dilation and the total AE events decreased with shear cycles because of the damage inflicted on asperities during the previous shear cycle. Two stages were observed in the normal displacement curves under low normal stress, whereas three stages (compression, dilation and compression again) were observed at a higher normal stress; the second compression stage may be caused by tensile failure outside the shear plane. The magnitude of the normal stress and the state of asperity are

two important factors controlling the post-peak stress drop and stick–slip of granite joints. Serious deterioration of asperities will stop stick–slip from recurring under the same normal stress because the ability to accumulate energy is decreased. The AE *b*-value increases with the number of shear cycles, indicating that the stress concentration inside the fault plane is reduced because of asperity damage; thus, the potential for dynamic disasters, such as fault-slip rockbursts, will be decreased.

Keywords Granite joints · Asperity damage · Acoustic emission · Dilatation · Stick–slip

1 Introduction

Rock masses are typically characterized by discontinuities, such as faults, joints, and other planes of weakness. Joints can significantly affect the mechanical behavior of rock masses and create pronounced anisotropy in the rock mass properties, such as its shear strength and rock permeability. Shear failure along the weak joints is one of the main failure modes in rock engineering, and many well-documented catastrophic disasters have been caused by slip along rock discontinuities in foundations, dams, tunnels and slopes. Thus, it is important to understand the frictional behavior of joints under shear loads. The mechanical behavior and shear strength of a rock joint are influenced by factors such as rock type, normal stress, shear rate, size of the joint, degree of weathering, presence of moisture, water pressure and surface roughness. Joint surface roughness has been recognized as one of the most important factors and has a significant impact on the mechanical behavior of joints (surface roughness influences not only the peak shear strength of the discontinuity but also the

✉ Fanzhen Meng
xuelianmfzh@163.com

✉ Hui Zhou
hzhou@whrsm.ac.cn

¹ College of Science, Qingdao University of Technology, Qingdao 266033, Shandong, China

² State Key Laboratory of Geomechanics and Geotechnical Engineering, Institute of Rock and Soil Mechanics, Chinese Academy of Sciences, Wuhan 430071, Hubei, China

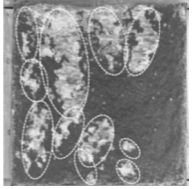
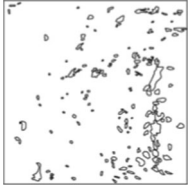
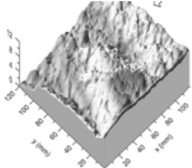
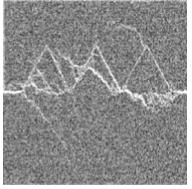
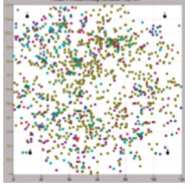
post-peak behavior, such as strain softening). Numerous laboratory and numerical investigations (Hutson and Dowding 1990; Huang et al. 1993; Pereira and de Freitas 1993; Wang and Scholz 1994; Karami and Stead 2008; Park and Song 2009; Asadi et al. 2012, 2013; Indraratna et al. 2014, 2015; Hong et al. 2016; Singh and Basu 2016) have described the asperity degradation/damage that can occur as a result of attrition and asperity breakage caused by over-stressing upon shearing.

Five methods are commonly used to investigate the asperity degradation of rock joints in the literature; these methods are listed and compared in Table 1. The simplest method is direct observation of the joint surface after shear failure; the failure zone can be distinguished from the undamaged surface both by its different color and by the powder and small fragments on the surface. However, this method provides only a rough evaluation of the damage. Researchers also use photo image analysis; in this method, images of the specimen surfaces are taken using a high-resolution digital camera, and the damaged asperities can be identified if they have different colors than the undamaged zones; moreover, the length, width and area of the degraded zone can be calculated (Hong et al. 2016). However, the difference in color between the joint surface and the damaged asperities is small for certain types of rock, and the color change attributable to asperity degradation under low normal stress is not obvious for hard rock such as granite; thus, it is difficult to define the extent of the damaged area for such materials. Three-dimensional (3D) laser imaging has been widely adopted to characterize the joint roughness (Grasselli et al. 2002; Grasselli and Egger 2003; Li et al. 2015; Singh and Basu 2016; Tang and Wong 2016). In addition, the asperity height, the dip angle and other statistical parameters can be obtained and used to quantify the asperity damage during shear. The above three methods can only be used when a shear test is completed. Moreover, real-time information about asperity damage during different stages of the shear process cannot be obtained. Numerical methods, such as PFC2D/3D, are also used to study the failure mechanism of rock joints (Cho et al. 2008; Karami and Stead 2008; Park and Song 2009; Asadi et al. 2012, 2013; Bahaaddini et al. 2013, 2016). Using these techniques, the macro-shear strength of different joints can be acquired; the micro-crack initiation and propagation process can be clearly observed throughout the shear process; and the proportion of shear cracks and tensile cracks can be determined. However, the properties of the microscopic constituents in PFC are typically not known, and a tedious calibration process of the micro-parameters is required to ensure that the macroscale response of the model corresponds with the laboratory test results. When brittle fracture occurs in rocks, elastic waves called AEs are emitted, which can be used to locate the fracture

events and analyze the intensity of the fractures. Based on the research by Li et al. (2015), the damaged zone on a joint surface corresponds to the steepest asperities of the joint facing the shear direction; the distribution of AE events is in agreement with that of the actual damage of a joint surface. Therefore, AE monitoring is a promising approach for determining the asperity damage at any moment in the shear process (Moradian et al. 2010, 2012).

Recently, not only the static stability of a jointed rock mass has been considered, but a need to assess dynamic stability has arisen because of an increased concern regarding earthquakes, rockburst and explosions (Lee et al. 2001; Sainoki and Mitri 2014a, b, 2015; Meng et al. 2016). Moreover, the cyclic shear and dynamic shear behavior of rock joints have become more important for understanding the natural phenomena of higher loading frequencies, and different models for asperity damage have been proposed under cyclic shear loading (Plesha 1987; Hutson and Dowding 1990; Huang et al. 1993; Qiu et al. 1993). Lee et al. (2001) conducted cyclic shear tests on marble and granite joints and concluded that the mechanism of joint degradation and the behavior of shear resistance are primarily attributable to the effect of second-order asperities and the strength of the rock material; the degradation of asperities under cyclic shear loading followed the exponential degradation laws for the asperity angle. Jafari et al. (2003) found that degradation of both first- and second-order asperities will occur during cyclic shear displacement depending on the cyclic displacement and normal stress applied. Sainoki and Mitri (2014a, b, 2015) performed dynamic modeling of mining-induced fault slip, finding that the magnitude of the stress drop resulting from asperity shear on a fault surface is a key factor determining the intensity of near-field ground motion induced by a fault slip. Meng et al. (2016) proposed a method based on the AE b -value to predict the rockburst hazard induced by structural plane shearing in deep tunnels under high geostress. The stick-slip of a fault plane has been recognized as a mechanism of shallow earthquakes (Brace and Byerlee 1966), and it was found that the stick-slip of a small-scale fault can also induce a fault-slip rockburst in deep tunnels and mines caused by violent energy release (Zou 1988; Zou et al. 1989; Tarasov 2014; Khosravi 2016; Meng et al. 2016). The temporal variation in the b -value (b -value can be calculated by the Gutenberg–Richter relation using seismic data or acoustic emission data) is a significant precursor of volcano activities and earthquake occurrences (Scholz 1968; Smith 1981; Chan et al. 2012), and many researchers have observed a decrease in the b -value in source regions prior to an earthquake (Nanjo et al. 2012; Nuannin et al. 2012; Wang et al. 2016). Moreover, regions with low b -values can be connected to fault-structural heterogeneity and local stress concentrations, which cause

Table 1 Summary of the five commonly used methods in joint asperity degradation study

No.	Method	Advantage	Disadvantage	Exemplification
1	Direct observation	Simple and intuitive	Only rough and qualitative analysis can be conducted; cannot be used if color difference between damaged and undamaged area is very small	 Indraratna et al. (2014)
2	Photo image analysis	Damaged area can be accurately and quantitatively measured	Only the damaged area can be measured, the degradation of asperity height cannot be evaluated; cannot be used if color difference of damaged and undamaged area is very small; can only be measured after the shear test	 Hong et al. (2016)
3	Laser scanning of morphology	Many parameters such as asperity height and dip angle can be accurately and quantitatively measured	Only geometric parameters of surface asperity can be obtained; can only be tested after the shear test, and the asperity parameters cannot be obtained in real time during shear	 Indraratna et al. (2014)
4	Numerical simulation such as PFC2D	Process of crack initiation, growth, coalescence, localization and complete breakdown can be visualized without requiring continuous system re-configuration; shear or tensile fracture can be differentiated	Parameter adjustment is complex and time consuming during modeling; there are some differences between the modeling result and the actual experimental result due because of the oversimplification of the model	 Asadi et al. (2013)
5	Acoustic emission (AE) source location	The damage and fracture can be located and the damage degree can be determined by analyzing AE event rate and energy rate at any moment during shear; shear or tensile fracture can be differentiated	Sometimes the location accuracy of the events is less than the aforementioned methods	 Moradian et al. (2012)

seismic events to increase to relatively larger sizes once they begin to nucleate (Schorlemmer and Wiemer 2005; Goebel et al. 2013).

The above analysis shows that it is fundamental and vital to study asperity damage because such investigations can provide the guidance and data necessary for the development of a quantitative theory and constitutive model for rock joint behavior. Although many studies have been devoted to investigating the effect of joint roughness on the shear behavior of rock joints, the mechanisms of asperity degradation in the shearing process are still not

well understood (Bahaaddini et al. 2013). Saw-toothed joints, replicas of natural joints or tensile joints of model material were mostly tested in previous studies; however, hard and brittle rocks are more suitable to investigate asperity damage and post-peak shear behavior under high normal stress. Although AE is a promising approach for detecting asperity damage during joint shear, only a few studies have addressed the application of this technique for monitoring the shear mechanism of rock joints under high normal stress.

In this study, tensile granite joints are sheared under a constant normal load, the damage characteristics of asperity are investigated based on the AE technique, and the influences of asperity damage on post-peak behavior and dilatation are discussed. The effects of asperity degradation on stick–slip that can result in fault-slip rockburst are analyzed; the b -values calculated by the Gutenberg–Richter relation during each shear are studied, and the impact of asperity damage induced by repeated shears on stress concentration on the fault plane is presented. The results of this study will contribute to the understanding of asperity damage and the shear mechanism of hard rock joints under high normal stress and could promote the application of AE techniques to monitor and warn of static or dynamic shear failure of in situ joints.

2 Specimen Preparation, Experimental System and Procedure

Cubic intact granite samples of 10 cm on each side were cut from a long piece of granite collected from a building material market and then ground to make the opposite faces parallel according to the suggested method of the International Society for Rock Mechanics (ISRM). Rough joint surfaces were created by splitting these blocks using an indirect tensile loading system (Brazilian testing method). Shear tests were conducted using an RMT150C testing machine at the Institute of Rock and Soil Mechanics, Chinese Academy of Sciences. The maximum normal and shear load values were 1000 and 500 kN, respectively. Shear stress was applied at a rate of 0.005 mm/s after a pre-set normal stress was exerted and kept constant. Acoustic emissions were monitored with a 16-channel PAC-DISP system, and four PICO sensors 0.5 cm from the joint surface were used to locate the AE events in the surface plane. The resonant frequency and operating frequency range of the sensors were 500 and 200–750 kHz, respectively, and the sampling rate was set to 1 million samples per second. The amplification of the preamplifier and the threshold of the system were both 40 dB. A layer of couplant was painted onto the interface of the rock and the piezoelectric ceramic of the sensor to reduce attenuation of the AE signals. The experimental setup, the acoustic emission system and the arrangement of the AE sensors are presented in Fig. 1.

In previous studies on shear behavior and the peak strength model of joints, the normal stress applied was usually low because such studies typically concentrated on shallow buried rock engineering projects, and model materials such as plaster and cement mortar were widely used. However, the burial depths of many tunnels exceed 2000 m, with high stress levels acting on the discontinuities. Therefore, the normal stress set in this study ranges

from 1 to 45 MPa (1, 3, 5, 7, 10, 20, 30, 40 and 45) to investigate the shear behavior of joints under different stress levels.

3 Results of the Shear Test on Granite Joints Under Constant Normal Load Conditions

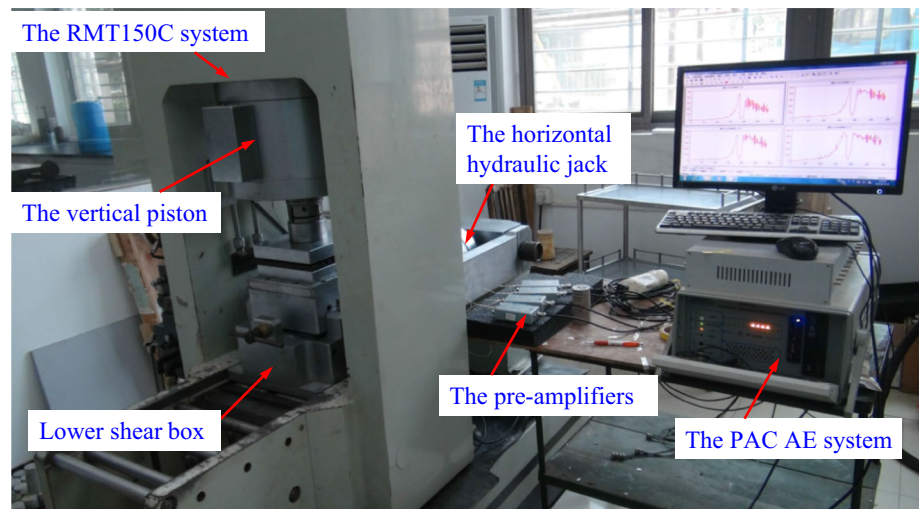
3.1 Shear Stress–Shear Displacement Curves

The plot in Fig. 2 shows the shear stress versus shear displacement curves of the granite joints. This figure shows that the level of normal stress has a significant influence on the shear strength curves of granite joints, and three types of curves can be distinguished. The first type of strength curve occurs when the normal stress is less than 3 MPa. In this curve, the shear stress gradually increases, and after the peak shear strength is reached, the stress slowly decreases to the ultimate shear strength. The joint shows strong brittle failure characteristics when the normal stress is greater than 5 MPa. The second type of strength curve occurs from 5 to 7 MPa. In this curve, the shear stress decreases drastically after the peak shear strength is reached and then increases again with shear displacement to a relative peak value before decreasing to the ultimate shear strength. The third type of strength curve occurs when the normal stress is greater than 10 MPa. In this curve, violent post-peak stress drops and periodic shear stress oscillations with instantaneous small shear stress drops (also termed stick–slips) occur simultaneously. All of the stress drops that occur during shearing were accompanied by a loud sound. These strong brittle failure characteristics of joints have rarely been reported in other studies either because joints made of model materials were used or low normal stress was applied for the real rock joint tested in the experiments, demonstrating the need to use real rock rather than model material to study the shear behavior of hard and brittle rock joint under high normal stress. The test result also indicates that no obvious yielding occurs in asperities even when normal stress is up to 45 MPa, which is different from intermediate hard or soft rock such as marbles, limestone and cement mortar that shear stress remains nearly constant rather than weakening after peak shear strength is reached under high normal stress. Similar results are also reported by Wawersik and Brace (1971), Tarasov and Randolph (2011), Meng et al. (2015) and Ai et al. (2016) that strong brittle failure occurs even under high confining pressure due to the brittle and stiff compositions (quartz, feldspar) of granite.

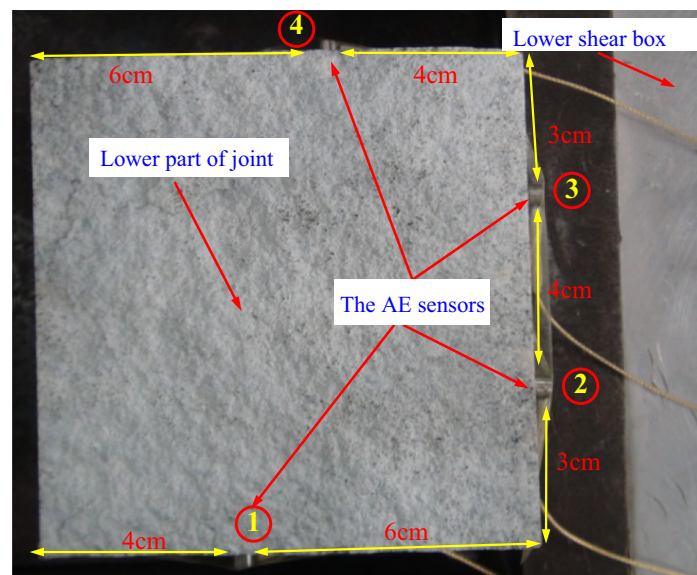
3.2 Distribution of AE Events of Joint with Normal Stress

The two-dimensional (2D) locations of AE events of joint surfaces were determined during shear. Figure 3 shows the

Fig. 1 Experimental setup (a) and arrangement of the AE sensors (b), the four sensors were within the same plane, which was 0.5 cm from the surface; the numbers in circles are number labels for the sensors



(a)



(b)

AE events under different normal stresses (the coupling interaction between the sensors and the rock face loosened as a result of rock deformation under high normal stress, so AE data from normal stress of only 1 to 20 MPa were obtained and analyzed). According to the definition of AE and the research results from other researchers, every AE event denotes a small-scale fracture in the rock. For the shear of a rock joint, the AE signals mainly come from the cracking, rolling, crushing and sliding of asperities on the surface, whereas a small portion stem from local fractures inside the intact rock away from the joint surface. The figures illustrate that the total number of AE events tends to increase with normal stress, indicating that the level of normal stress has a considerable impact on the damage of surface asperities, with the degree of asperity degradation increasing with normal stress. Because the joints used in

this study have different surface morphologies, not all of the joints conformed to the rule that events increase with normal stress, indicating that asperity damage is dependent on not only the normal stress but also the surface morphology of joints.

4 Characteristics of Asperity Damage Based on AE Events Under Different Normal Stresses

Figure 4 shows the cumulative AE events and shear stress with shear time under different normal stresses; the event curve was approximately in the shape of an “S,” and three stages could be determined: a slow increase stage in the initial shear, a rapid growth stage in the intermediate shear and a slow increase stage (or nearly constant) at the end of

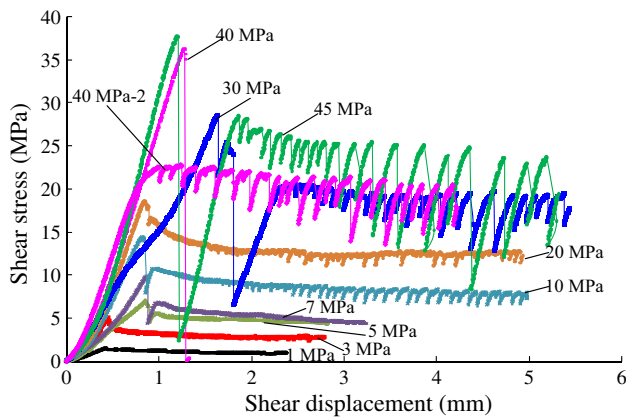


Fig. 2 Curves of shear stress versus shear displacement for granite joints (peak stress dropped to 0 from 36 MPa for granite joint when the normal stress was 40 MPa, and a loud sound was emitted; the 40 MPa 2nd curve is the curve for the same joint after the second shear)

shear. Because granite is a hard rock composed of hard brittle minerals, such as quartz, feldspar and mica, the AE remains active as a result of the rolling, crushing and sliding of brittle minerals in the final sliding stage, resulting in the second turning point (transition point from rapid growth to slow growth) in the event graph being inconspicuous for some cases. The rapid growth of AE events indicates that the damage of asperities is aggravated by continuous shear; thus, the first turning point in the cumulative event curve (i.e., the transition point from slow growth to rapid growth) is defined as *asperity damage initiation shear stress* (τ_{di}) in this study. The τ_{di} values of the joints when the normal stress was 1, 3, 5, 7, 10 and 20 MPa were calculated based on the cumulative AE event curves and are listed in Table 2. It can be seen that τ_{di} of all of the joints is approximately 0.5 of peak shear strength, presenting weak relationships with normal stress. The criterion for *asperity damage initiation shear stress* can be summarized as follows:

$$\tau_{di} = 0.485\tau_p$$

Thus, if the peak shear strength criterion is established, the *asperity damage initiation shear stress* can be determined using the above formula.

The number of AE events in the three stages from the starting point to damage initiation shear stress to peak shear stress and to the end of the test was obtained to analyze the AE event at different stages during shear. To investigate the unstable stick–slip behavior, the total shear displacement of joints under high normal stress is greater than under low normal stress, and the number of AE events increases with displacement. Thus, for comparison, we only counted the AE events from 0 to 2.5 mm (0 to 500 s) of shear displacement or shear time (because the least shear

displacement is 2.5 mm, which is obtained when normal stress is 1 MPa); the statistics are also given in Table 2, N_{di} , N_p and N_t are the number of AE events at the asperity damage initiation shear stress, peak shear strength and terminal point of the statistics (i.e., 500 s). According to the analysis, only a few AE events—fewer than 10% or even 5% of the total events (N_{di}/N_t)—are generated in the first stage, indicating that only position adjustments and elastic compaction of asperities occur and the damage of asperity is extremely limited. After asperity damage initiation shear stress is reached, the degradation rate dramatically increases and the number of AE events accounts for 10–30% of the total events [$(N_p - N_{di})/N_t$] in the second stage, illustrating that total damage remains low even though the damage rate is faster. Massive asperity damage occurs beginning at peak shear strength in the third stage because 63–85% of the total events [$(N_t - N_p)/N_t$] are generated during this period. The above analysis shows that the damage has the following characteristics: a small amount of damage occurs before τ_{di} at a very slow rate; the damage was aggravated with a higher rate from τ_{di} , and the majority of the damage occurred after the peak shear strength, with a slightly lower rate than in the prior stage. These damage characteristics, obtained from the AE events distribution, are consistent with both the conclusion of Grasselli et al. (2002) and the numerical results of Karami and Stead (2008) and Bahaaddini et al. (2013). Brittle failure occurs and peak strength drops to a low value under moderate or high normal stress; next, the shear stress increases again, which can be treated as a reloading process. Therefore, the damage rate decreases during this time, which is why a small plateau emerges on the cumulative event curve.

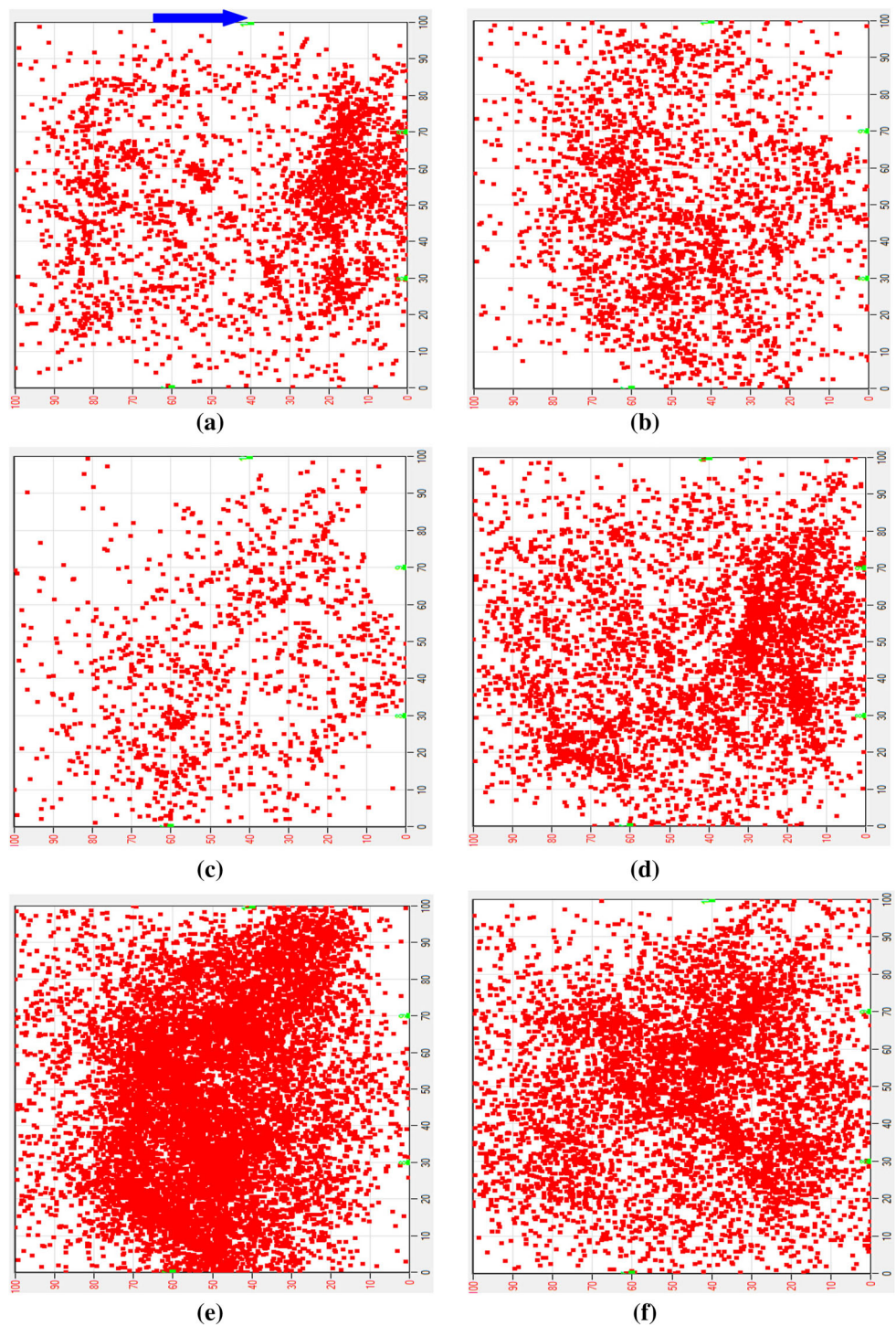
5 Dilatation Characteristics and Evolution of AE Events of Granite Joints with Shear Cycles

5.1 Dilatation Characteristics of the Granite Joints

Joint roughness increases the shear strength of a rock mass, particularly in an underground environment, where dilation of the rock along the joint surface is partially or completely constrained. Under this condition, normal stress on the joint surfaces increases, leading to the closure of open joints and substantially higher joint shear strengths (Karami and Stead 2008). Thus, different peak dilation angle models were proposed, based on which various peak shear strength criteria were established. Moreover, the damage of asperities can be analyzed by studying the dilation curves because the dilation phenomenon may be prominent when the asperities are intact and without damage, whereas dilation may be weakened if the asperities are cut off and

Fig. 3 Distribution of AE events for granite joints under different normal stresses during the entire shear process:

a 1 MPa, **b** 3 MPa, **c** 5 MPa, **d** 7 MPa, **e** 10 MPa and **f** 20 MPa (the four green points in each figure are the four sensors; the arrow indicates the shear direction)



seriously damaged. Therefore, there is not only theoretical significance but also practical significance to investigating the dilatation characteristics of granite joints.

Because the curve patterns differ significantly, the normal displacement versus shear displacement diagrams when the normal stress is 1, 3, 5, and 7 MPa and 20, 30, 40, and 45 MPa were separated and are shown in Fig. 5a, b, respectively.

When the normal stress is lower than 7 MPa, the normal displacement curves can be divided into two stages, which are separated by the dotted line in Fig. 5a. At the initial stage of shear, the normal (vertical) deformation is compression; after the maximum vertical displacement is reached, the joint begins to dilate until the end of the test. Furthermore, the dilatation curves illustrate that the vertical displacement (the dilatation part) increases at a slower rate

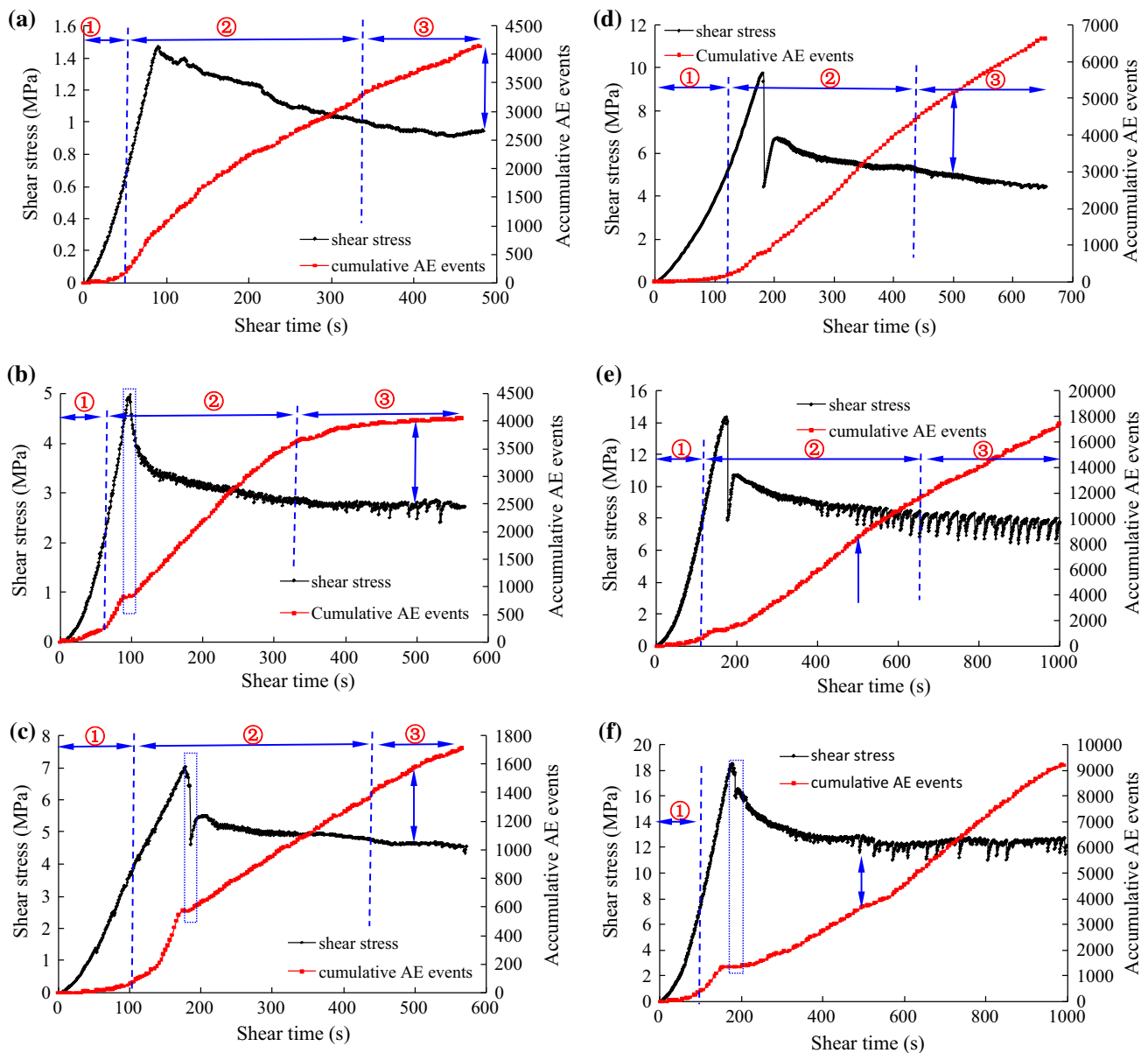


Fig. 4 Cumulative AE events and shear stress with shear time under different normal stresses: **a** 1 MPa, **b** 3 MPa, **c** 5 MPa, **d** 7 MPa, **e** 10 MPa and **f** 20 MPa (the vertical arrows indicate the terminal

point of AE statistics, i.e., 500 s, and the dotted boxes show the small plateau; ①, ② and ③ indicate slow increase stage, rapid growth stage and slow increase stage of AE events, respectively)

with shear displacement and that the curve nearly remains constant when the shear displacement exceeds 1.5 mm under a normal stress of 7 MPa. Moreover, the maximum normal displacement (dilation) tends to decrease with normal stress.

Normal displacement for joints under normal stress of higher than 20 MPa undergoes three stages with shear displacement, as shown in Fig. 5b; the first two stages are similar to those under low normal stress, transforming from compression to dilation with increasing shear displacement. The test is artificially terminated after the dramatic post-peak stress drop when the normal stress is 40 MPa;

thus, the curves only show the first two stages (compression–dilation). Because the granite joint exhibits the strong brittle failure characteristic in the post-peak stage (the violent stress drop and periodical stick–slip), the curves skip when stress drops occur. Because the stress drops when the normal stress is 20 MPa are not dramatic, the dilation curve is considerably smoother than the other curves. The deformation becomes compressive from the second turning point (indicated by the dotted line with the same color as the corresponding normal displacement curve) on the curve, and the final compressive deformation tends to increase with normal stress.

Table 2 Statistics of shear strength and AE events under different normal stresses

σ_n (MPa)	τ_p (MPa)	τ_{di} (MPa)	τ_{di}/τ_p	N_{di}	N_p	N_t	N_{di}/N_t	N_p/N_t	$(N_p - N_{di})/N_t$	$(N_t - N_p)/N_t$
1	1.48	0.737	0.498	239	907	4152	0.0576	0.2184	0.1609	0.7816
3	4.98	2.28	0.458	277	822	4000	0.0692	0.2055	0.1363	0.7945
5	7.04	3.72	0.528	91	573	1572	0.0579	0.3645	0.3066	0.6355
7	9.77	5.08	0.520	181	787	5180	0.0349	0.1519	0.1170	0.8481
10	14.35	7.09	0.494	509	1239	8389	0.0607	0.1477	0.0870	0.8523
20	18.50	7.59	0.410	400	1367	3700	0.1081	0.3695	0.2614	0.6305

σ_n , τ_p , τ_{di} are normal stress, peak shear strength and asperity damage initiation shear stress, respectively; N_{di} and N_p are the number of AE events at the asperity damage initiation shear stress and peak shear strength, and N_t is the total number of AE events in the range of statistics, i.e., from shear displacement of 0 to 2.5 mm

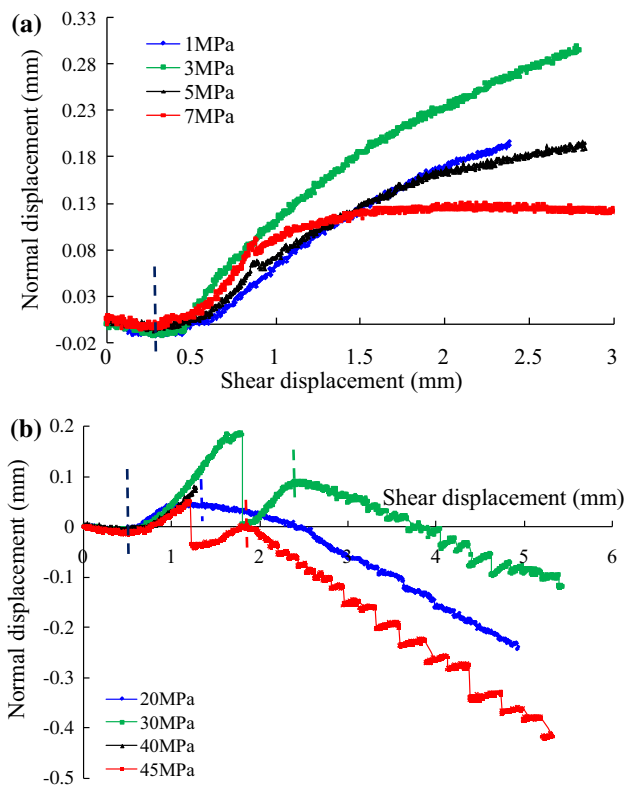


Fig. 5 Normal displacement–shear displacement diagrams for different normal stresses: **a** 1, 3, 5 and 7 MPa, **b** 20, 30, 40 and 45 MPa

Because rock slopes, large dam foundations, and underground rock structures, such as radioactive waste repositories and energy storage caverns, require a higher standard of stability against blasting and earthquakes, the cyclic shear and dynamic shear behavior of rock joints become more important for understanding the natural phenomena of higher loading frequencies. Rock joints may be sheared repeatedly when they are subject to cyclic loading, and because asperities on the joint surface may be damaged after the first shear cycle, the shear behavior may change considerably. Thus, some joints in this study are

repeatedly sheared, and the dilation curves that can reflect the degree of asperity damage are analyzed in detail.

After the first shear, the upper part of the joint was replaced at its location on the lower part as it was first sheared, then it was sheared along the same shear direction as the first shear under the same normal stress at the same shear rate. A portion of the normal displacement curves of granite joints undergoing 2 or 3 shear cycles under different normal stresses are illustrated in Fig. 6. The vertical displacement consists of compression and dilation if the applied normal stresses are not very high (such as 1 and 5 MPa in Fig. 6a, b) regardless of the shear cycles, and the increasing rate of vertical displacement decreases with the shear displacement; the second half of the curves become nearly horizontal. However, the maximum dilation value decreases and the dilation tends to transit to compression with an increasing number of shear cycles. Figure 6c, d illustrate that nearly no dilation occurs during the second shear cycle when normal stress is high (here, 20 and 30 MPa), a result that is different from joints sheared under low normal stress, as shown in Fig. 6a, b. The maximum compressive displacement also increases with the number of shear cycles.

At the initial stage of shear, the gap between the two surfaces is gradually closed and elastic compressive deformation of the contacting asperities occurs; thus, vertical compressive deformation occurs. When these compressed asperities are about to slide onto one another, the vertical deformation transforms from compression to dilation; this continues until the end of the test, when the normal stress is low (such as a normal stress of 1, 3 or 5 MPa). However, the dilation can remain nearly constant during the final stage of shear under a higher normal stress because the degradation of the asperity has reached its limit, and no compression or dilation will proceed. Moreover, the dilation will shift back to compression when the normal stress is higher than 20 MPa. The above analysis demonstrates that the initial compression is caused by

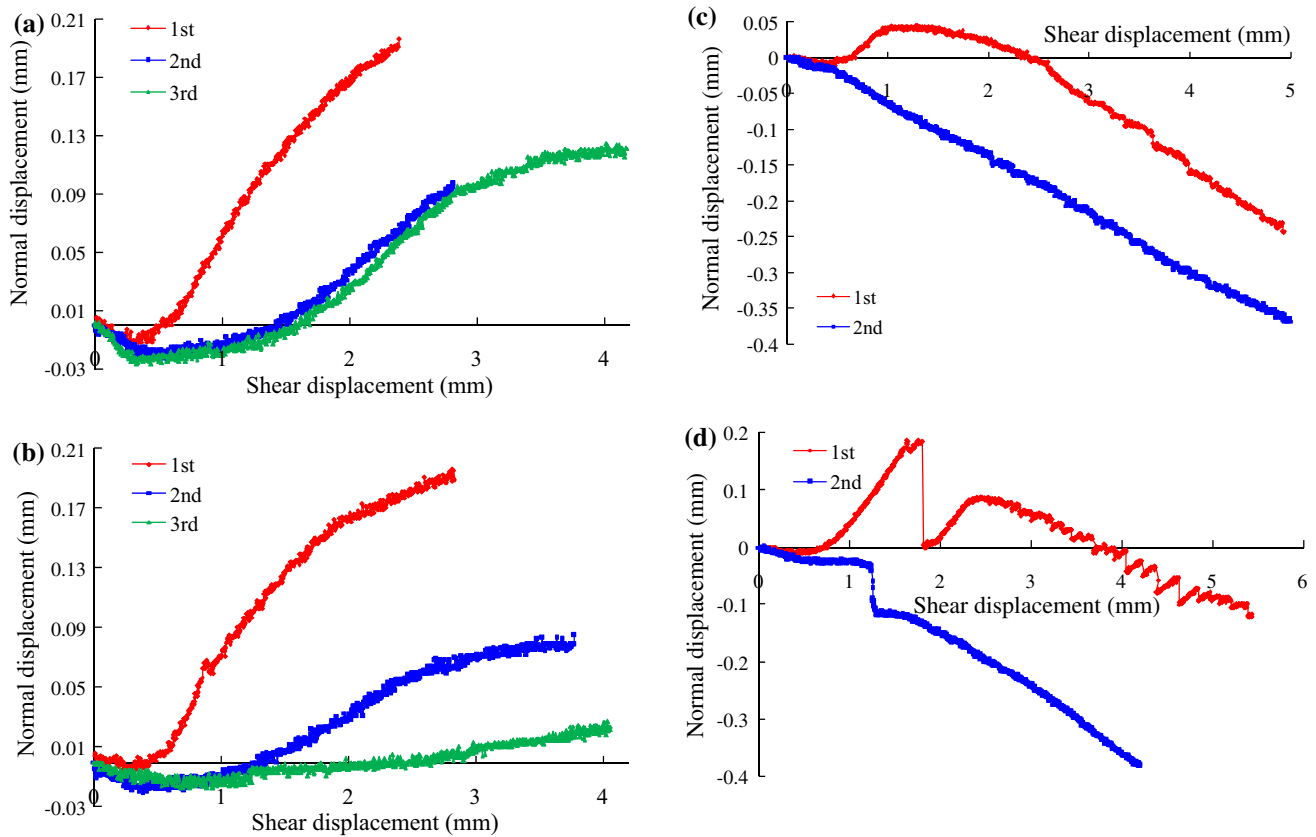


Fig. 6 Normal displacement versus shear displacement diagrams for granite joints that underwent 2 or 3 shear cycles: **a** 1 MPa, **b** 5 MPa, **c** 20 MPa and **d** 30 MPa

closure of the aperture and part of the elastic deformation and that the intermediate section of dilation is caused by the uplift effect when asperity overriding and sliding occur. A careful inspection of the specimen after failure indicated that compressive deformation in the last stage of the normal displacement curve with high normal stress arises from internal damage and tensile cracking in the specimen. A typical photograph of the specimen is shown in Fig. 7; in addition to the asperity abrasion and damage on the joint surface, failure occurs outside the shear plane and some oblique fractures appear on the upper and lower parts of the intact rock, which intersect with the shear direction at an acute angle. These fractures have also been reported by other researchers (Karami and Stead 2008; Asadi et al. 2012, 2013; Bahaaddini et al. 2016) in a numerical study and are caused by the shear and tensile stress concentrated along the fracture surface, particularly at the root of large asperities. Micro-cracks are initiated once the tensile strength of the asperities is exceeded and extend to form long tensile fractures. As stated by Asadi et al. (2013), normal stress must be higher than a critical value to see failure develop outside the shear plane. Sliding will occur for normal stresses below this critical value. After these

tensile cracks are generated, the vertical compressibility of the joints increases.

With an increasing number of shear cycles, the steep asperities are degraded and the crushed particles fill in the small valleys between asperities; thus, vertical dilation is weakened. The dilation is primarily caused by the overriding and sliding of the contact asperities, and when a joint is sheared under low normal stress, the large-sized asperity cannot be sheared off; thus, the aperture between the opposite surfaces becomes wider as shear proceeds and the dilation is prominent. With increasing normal stress, a portion of the asperities can be cut off during shear, leading to a smaller uplift magnitude and thus reduced dilation.

5.2 Evolution of AE Events with Shear Cycles

The extent of asperity damage can be reflected by the number and distribution of AE events; thus, the evolution of AE events with shear cycles is presented in this section.

Table 3 provides the number of located AE events for these joints, which underwent several cycles of shear. During the 1st, 2nd and 3rd shear, 4152, 2149 and 1833 events were recorded, respectively, under 1 MPa of normal

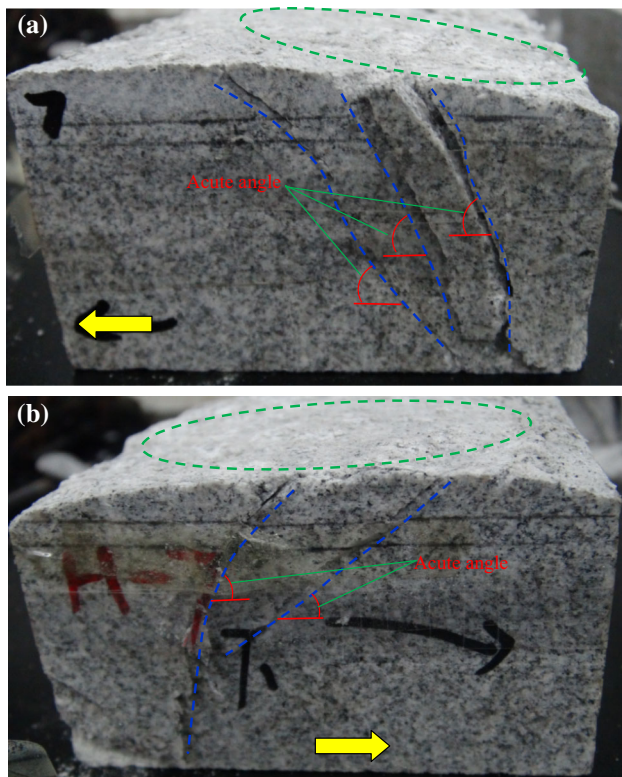


Fig. 7 Photographs of a joint after the second shear under 40 MPa of normal stress; **a** and **b** are the left and right of the lower part, respectively, and the arrow indicates the shear direction; the green and blue dotted lines show the surface damage and the tensile fractures in intact rock, respectively

stress. Figure 8 shows the distribution of the AE events in the shear process (for comparison, the total shear displacement (or shear time) for different shear cycles under the same normal stress should be equal, as listed in Table 3). The change patterns of the AE events with the number of shear cycles are consistent with the dilation characteristic discussed in Sect. 5.1, and the bulk of the asperities were degraded during the first shear; thus, the AE events and magnitude of dilation decreased during the second shear. In the third shear, fewer AE events and less dilation occurred because of the repeat damage process in the second shear. For a normal stress of 5 MPa, 1709, 1360 and 960 events were obtained in the three shear cycles.

Table 3 Statistics of AE events under different normal stresses that have experienced several shear cycles

Normal stress (MPa)	Total shear displacement (mm) or time (s)	Number of AE events		
		1st	2nd	3rd
1	2.39 (488)	4152	2149	1833
5	2.83 (566)	1709	1360	960
7	2.90 (582)	6012	2719	2057
10	4.98 (1017)	17,464	18,364	/

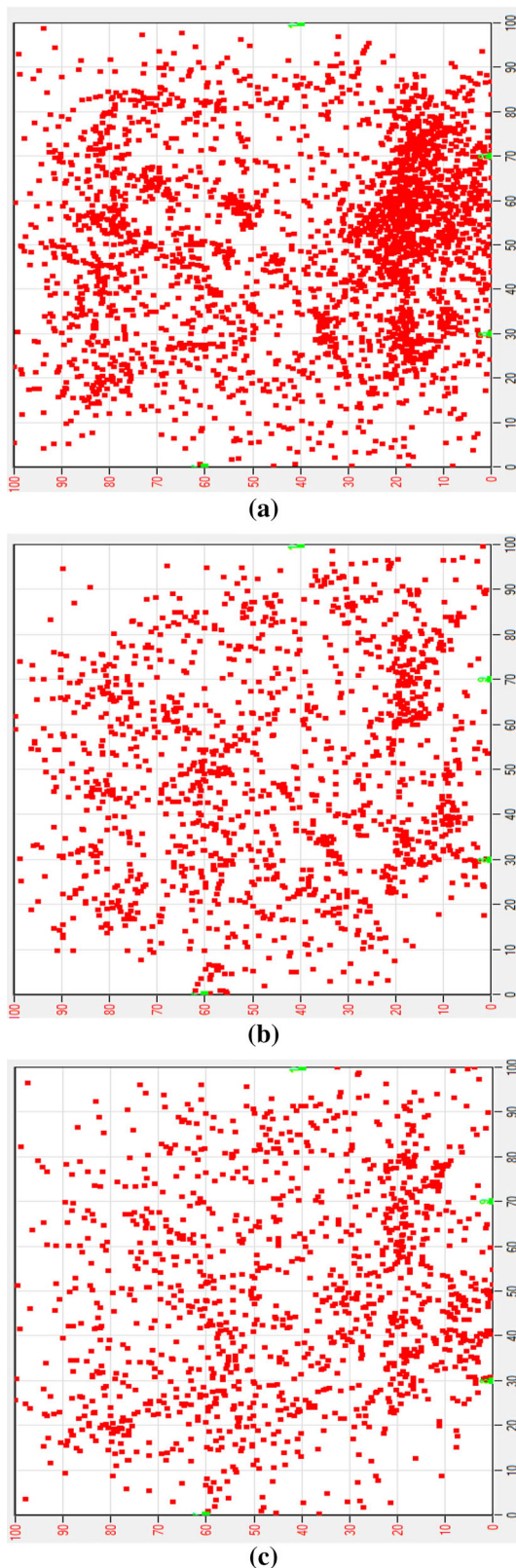
The above analysis and data in Table 3 indicate that both the dilation curves and the evolution of AE events with shear cycles can reflect the damage and degradation of surface asperities. The distribution of AE events can reflect the degradation of asperities on the joint surface, and the dilation curves can represent both the degradation of surface asperities and damage such as the tensile fracture within the upper and lower intact rock. After the first shear, the steep asperities or the tip of the asperity are cut off, weakening the dilation in the subsequent shear cycles. The majority of the asperities fail because micro-cracks are subjected to shear and tensile stress and AEs are radiated. However, when asperities are sheared off and destroyed, AEs mainly result from rolling and crushing of the debris and sliding friction between the contact surfaces.

6 Influence of Asperity Damage on the Shear Behavior of Rock Joints

When shear displacement occurs between the two interfaces of a joint, the asperities on the surface are degraded because of abrasion or cutting off. The joint can also be subjected to cyclic shear caused by earthquakes and blasting dynamic load, and the asperities can be repeatedly damaged. In this section, shear behavior, including shear stress curves, shear strength, stick–slip and the AE *b*-value of the granite joint, which has undergone several shear cycles, is presented and analyzed.

6.1 Effect of Asperity Damage on the Post-peak Shear Behavior of the Joints

Figure 9 shows the curves of shear stress versus shear displacement of the granite joints under different normal stresses and subjected to several shear cycles. The granite joints are characterized by strong brittle failure with increasing normal stress, and no post-peak stress drop occurs when the normal stress is 1 MPa. The obvious peak shear strength disappears and the shear stress remains nearly constant after the turning point is reached during the second and third shear cycles for all joints. Furthermore, the ultimate shear strength in the first shear (although periodic stick–slip occurs in the ultimate sliding stage, the



◀**Fig. 8** Distribution of AE events for a granite joint that underwent several shear cycles under a normal stress of 1 MPa; **a**, **b** and **c** are after the first, second and third shears, respectively (for comparison, the statistical range of AE events is from beginning of the shear test to shear displacement of 2.39 mm, which is the least among three cycles)

maximum stresses during each small stress oscillation are nearly equivalent and are connected by the green dotted line in each figure; this stress is treated as the ultimate shear strength) is nearly the same as that in the subsequent shear cycles, except when the normal stress is 20 MPa, the shear stress gradually increases with shear displacement, as shown in Fig. 9e. It was found that two nonpersistent fissures had occurred at the two corners of the lower joint part after the first shear when normal stress is 20 MPa. After the second shear, two fragments are detached from host rock outside the fissures. Thus, the gradual increase in shear stress with displacement is caused by the increase in normal stress during shear (the normal load is kept at 200 kN, whereas the shearing area is reduced because of the exfoliation of two rock fragments; thus, the normal stress increases).

The above analysis clearly demonstrates the influence of asperity damage on the post-peak shear behavior of granite joints. When first applied, shear stress is mainly borne by these asperities facing the shear direction, with an apparent dip angle larger than a critical value (Grasselli 2001); only small asperities or the tips of large asperities are cut off if normal stress is low, and large asperities can be sheared off when high normal stress is applied. Energy accumulates in the locked asperities before the peak shear stress is reached, and larger asperities under higher normal stress accumulate more energy. After the peak shear stress when shear dislocation occurs, stress and energy are released in a slow (normal stress of 1 MPa) or abrupt (normal stress higher than 5 MPa) manner, depending on the level of the normal stress, which can also be induced from the distribution of AE events introduced in Sect. 4, in which most AE events are generated after the peak stress. When a joint is repeatedly sheared, energy cannot accumulate as before because of damage to the asperities, and the peak shear strength is determined by the friction strength between the interfaces, which differs only slightly from the ultimate shear strength in the first shear. Thus, the ultimate shear strength between different shear cycles is nearly identical.

6.2 Effect of Asperity Damage on Stick–Slip

There is no exception in which stick–slip occurs in the frictional sliding period when the normal stress is higher than 10 MPa in the first shear. In the second shear,

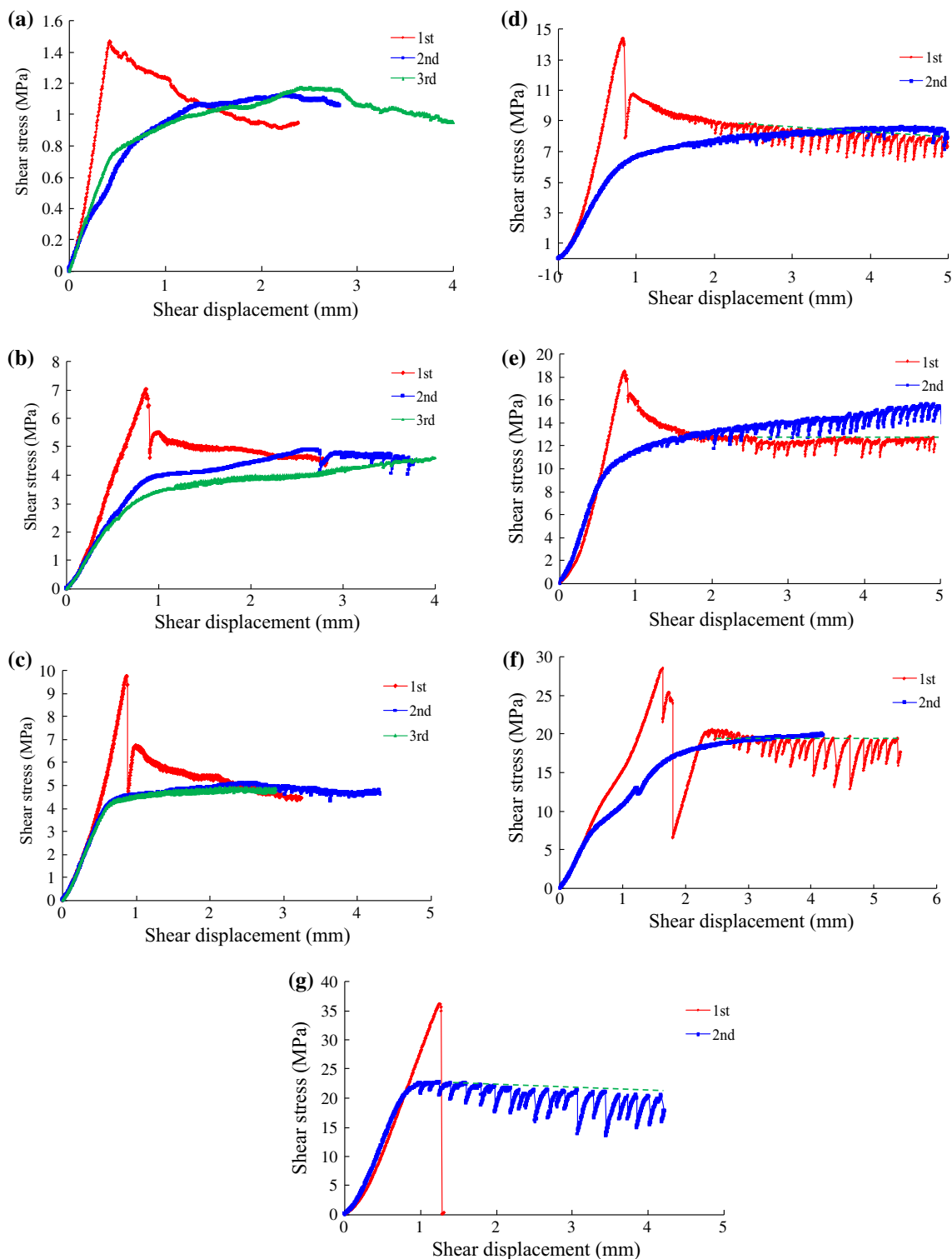


Fig. 9 Shear stress versus shear displacement curves of granite joints that underwent 2 or 3 shear cycles under different normal stresses: **a** 1 MPa, **b** 5 MPa, **c** 7 MPa, **d** 10 MPa, **e** 20 MPa, **f** 30 MPa and **g** 40 MPa

however, stick–slip only occurs for joints under normal stresses of 20 and 40 MPa; moreover, the shear behavior of the other joints in the second shear behaves the same as under low normal stresses, such as 1 and 5 MPa.

Although the dramatic post-peak stress drop and stick–slip (periodical stress drops) occur under a normal stress of 10 MPa in the first shear, no visible cracks and fissures are found on the two parts of the joint, except the asperity

damage on the surface, as shown in Fig. 10a, b. The green dotted box shows an area with serious abrasion and damage on the surface, which corresponds well with the area of dense distribution of AE events in Fig. 3e. During the second shear, the stick–slip disappears and no visible fissures arise on the specimen, as shown in Fig. 10c, d, indicating that no more fractures occur except for the further abrasion of the contact surface (areas of the white regions increase from Fig. 10a–d). The above analysis illustrates the important role played by the asperities in controlling the stick–slip in granite joints. Before the second shear begins, serious damage occurs to the surface asperities under a normal stress of 10 MPa; because stick–slip is a process of energy accumulation and release, the damages of the asperities make it difficult to build up a sufficient amount of energy to generate stick–slip.

When the normal stress is 30 MPa, the specimen after the first shear is as shown in Fig. 11a, b; one fissure with two branches nearly perpendicular to the shear direction can be seen on the upper part, which did not break down and remains integrated. Moreover, several minor cracks can be observed on the two edges of the lower part. After the second shear, more serious damage occurs on the two

parts of the joints, as shown in Fig. 11c, d; the upper part is still integrated, but some small thin-slabs on the two sides of the lower part fall apart from the host rock. Figure 11e, f show photographs of the two parts after the second shear. Several oblique tensile fractures that are clean and fresh can be seen on the left and right sides, indicating that in addition to the damage on the joint surface, the cracks that initiated from the root of asperities propagate to the inside of the specimen. As explained in the case of 10 MPa of normal stress, the damage to the surface asperities may prevent stick–slip from occurring because energy fails to accumulate in the damaged asperities. Another possible reason for the disappearance of stick–slip in the second shear cycle is that the fractures and fissures outside of the shear plane reduce the integrity of the joint, decreasing the ability to accumulate energy inside the upper and lower parts of the joint. However, as stated in Sect. 6.1, the ultimate shear strength (or peak shear strength, as they are nearly equivalent) during the second or third cycles of shear is nearly identical to that of the ultimate strength in the first shear, which is a general rule for joints regardless of the normal stress level. Only surface asperities occur under low normal stress, whereas asperity degradation and

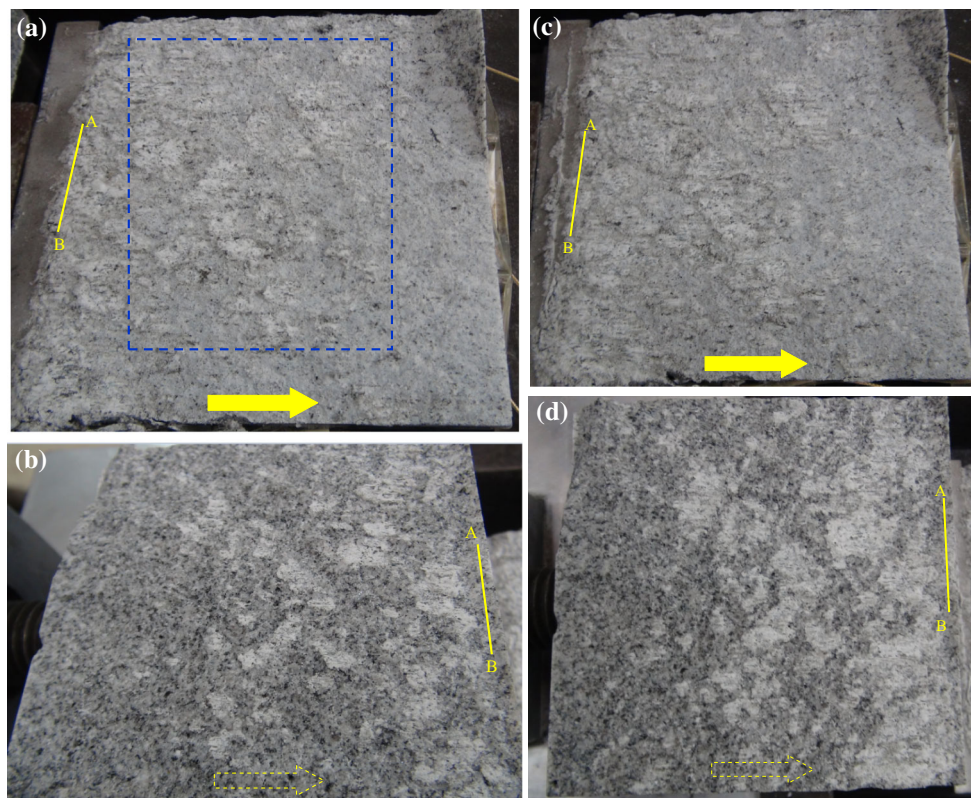


Fig. 10 Photographs of a joint after shearing under 10 MPa of normal stress; **a** and **b** are the lower and upper parts after the first shear, respectively, and **c** and **d** are the lower and upper parts after the second shear, respectively. The solid yellow arrow indicates the shear

direction of the lower part, and because the upper part is stationary in the shear direction, the dotted arrow indicates the relative shear direction

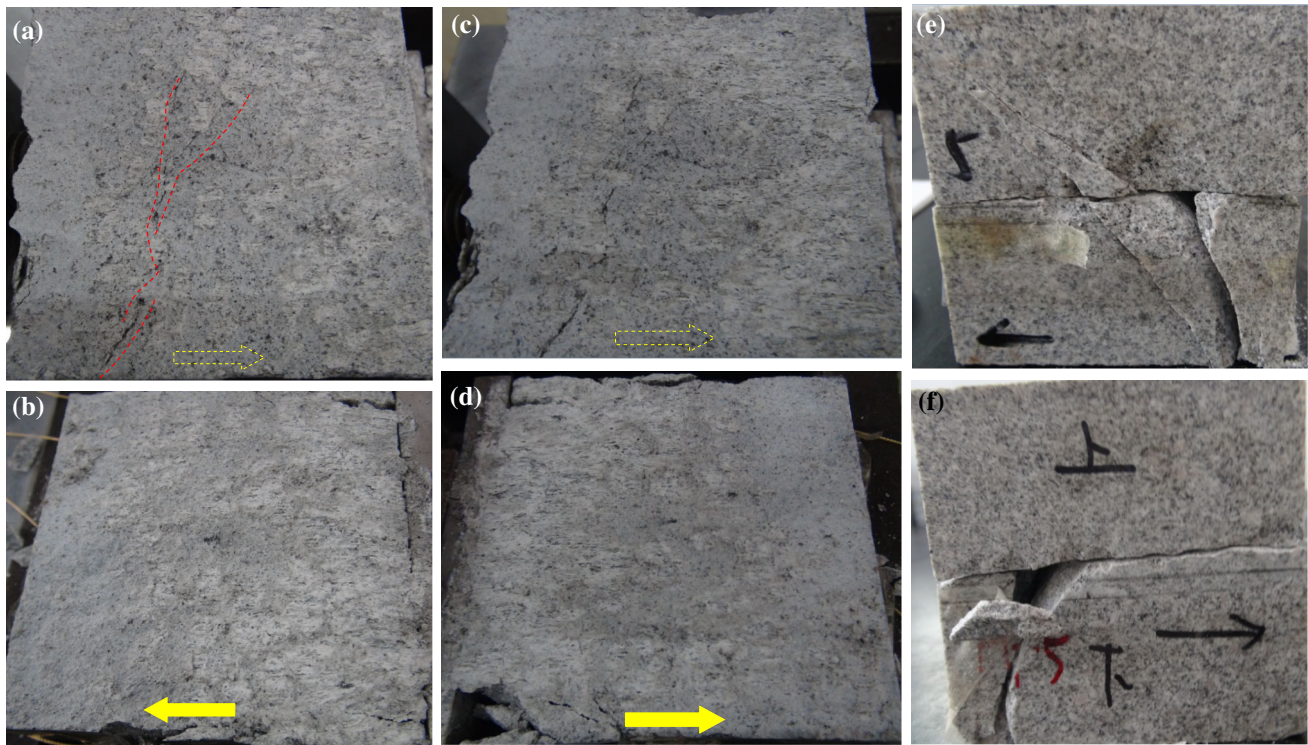


Fig. 11 Photographs of a joint after shearing under 30 MPa of normal stress; **a** and **b** are the upper and lower parts after the first shear, respectively; **c** and **d** are the upper and lower parts after the

second shear, respectively; and **e** and **f** are the right and left sides of the specimen after the second shear, respectively

tensile fracture outside the shear plane occur under high normal stress; they all correspond to the aforementioned rule, indicating that the tensile fractures may exert only a slight influence on the frictional behavior of joints. Thus, asperity degradation may be the primary reason to stop stick–slip from recurring.

The other two joints, sheared under 20 and 40 MPa of normal stress, behave differently than the two joints mentioned above, in which stick–slip occurred when sheared in the second cycle. As noted above, the gradual increase in shear stress during frictional sliding is caused by the decrease in shear area, increasing the actual normal stress that acts on the joint for the joint undergoing 20 MPa of normal stress. Similarly, it is likely the gradual increase in normal stress that leads to the stick–slip in the second shear of the cycle. Our study clearly shows that the magnitude of the normal stress has a considerable impact on stick–slip, which starts to appear only when normal stress is higher than 10 MPa, and that the average amplitude of stick–slip also increases with normal stress, as shown in Fig. 2. Stick–slip may occur after the joint sheared under 10 MPa of normal stress is re-sheared under 20 MPa or higher of normal stress.

The shear stress curve of the joint under 40 MPa of normal stress in the first shear is different from that of the other joints. A sharp drop in stress accompanied by a loud

sound occurs at the moment of peak strength. Because the failure process is so dramatic (the stress falls sharply from the peak value to 0), we immediately stop the experiment to examine and check the loading setup and specimen. The shear displacement is approximately 1.3 mm when the test is stopped, which is far less than the displacement for the other joint in the first shear mentioned above. Figure 12a, b shows the upper and lower parts of the joint after the first shear, respectively; there are no visible fissures on the two parts, indicating that the dramatic decrease in stress is mainly caused by cutting off brittle and hard asperities. Then, the shear test is restarted after the upper part is repositioned to its initial location under the same normal stress until a shear displacement of 4.3 mm is reached. Just as the other joints sheared twice, shear stress becomes nearly constant after the turning point (as shown in Fig. 9g); however, notable stick–slip appears during the frictional sliding period. Figure 12c, d shows the upper and lower parts of the joint after the second shear, respectively. A comparison of the upper part of the joint in Fig. 12a, c indicates that the white regions in Fig. 12a are not obvious and are considerably fewer in number than those in Fig. 12c; similarly, many more powder and white regions can be observed in Fig. 12d than in b in the lower part of the joint, indicating that limited damage has occurred on the asperities during the first shear because of the short

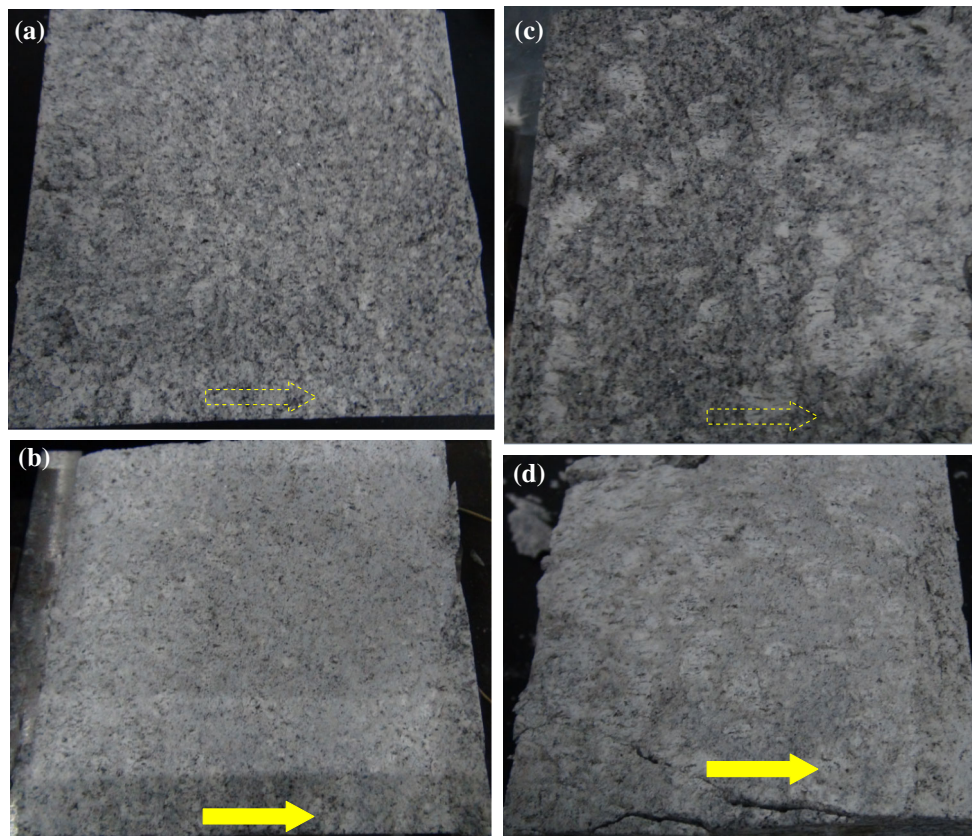


Fig. 12 Photographs of a joint after shearing under 40 MPa of normal stress; **a** and **b** are the upper and lower parts after the first shear, respectively, and **c** and **d** are the upper and lower parts after the second shear, respectively

shear distance. Thus, these undamaged or slightly damaged asperities can still play a significant role in controlling shear behavior (for example, the stick–slip in the second shear cycle), particularly when the shear displacement is in the range of 1.3 to 4.3 mm.

The above analysis shows that the level of normal stress and the state of asperity are two important factors that control the stick–slip of granite joints. Shear behavior of joints under normal stress of 10 and 30 MPa demonstrates that the degradation of asperities during the first shear will stop stick–slip from recurring in the second shear under the same normal stress because the ability to accumulate energy is decreased after serious deterioration of the asperities. Joints under 40 MPa normal stress illustrate that undamaged or slightly damaged asperities can still lead to stick–slip in the second shear under the same normal stress. Joints under 20 MPa normal stress show that stick–slip can also occur if a joint without stick–slip occurrence is re-sheared under higher normal stress. Stick–slip can only occur when normal stress is higher than a critical value regardless of whether the joint is in the first or second shear, and if the joint is sheared repeatedly, the critical value may be higher than its initial shear because it is easier to accumulate energy in the latter case.

6.3 Effect of the Shear Cycle on the AE b -Value

Gutenberg and Richter (1944) proposed an important frequency–magnitude (F – M) law for earthquakes in the form $\log N = a - bM$, where M is the earthquake magnitude and N is the cumulative frequency of the events with magnitudes $\geq M$. This law is hereafter denoted the GR law, and the b -value is an important parameter representing seismicity. The geometric meaning of the slope of the frequency–magnitude distribution demonstrates that a smaller b -value corresponds to a greater number of larger-magnitude earthquake events; thus, the b -value reflects the proportion of large-magnitude earthquakes relative to small-magnitude earthquakes.

Because of the similarity between natural earthquakes and the fracture or unstable sliding of rocks, the frequency–magnitude relationship for micro-fracturing events in the rock has been found to be the same as that for earthquakes, i.e., the frequency is a power function of the maximum trace amplitude, and one formula commonly used in the fields of concrete fracture and rock mechanics is as follows:

$$\log_{10} N = a - b \frac{A_{dB}}{20}$$

where A_{dB} is the peak amplitude of the AE events in decibels, $A_{dB} = 10 \log A_{max}^2 = 20 \log A_{max}$, and A_{max} is the peak amplitude of the AE events in millivolts (Colombo et al. 2003; Rao and Lakshmi 2005; Nejati and Ghazvinian 2014; Meng et al. 2016). Because earthquakes in the earth’s crust and fault-slip rockburst in deep tunnels are both dynamic disasters caused by unstable frictional slips (such as dramatic post-peak stress drops and stick–slips) of large- or small-scale faults, it will be very important to study the characteristic of the b -value to clarify the preparation process and the prediction of earthquakes and fault-slip rockbursts. This section discusses the effect of shear cycles on the AE b -value.

Only AE hits with peak amplitude higher than the threshold, which was set to 40 dB, are recorded by the AE sensor, so the range of the amplitude of AE signals is from 40 to 100 dB. Figure 13 shows amplitude distribution of AE hits captured by the four sensors when normal stress is 10 MPa in the first shear cycle. The first column in blue in Fig. 13a indicates that the number of AE hits with a maximum amplitude higher than 40 dB was 164,995, and the last blue column indicates that the number of AE hits with a maximum amplitude larger than 95 dB was 871. Then, $A_{dB}/20$ and $\log_{10}N$ were used as the abscissa and ordinate, respectively, to plot a series of data points in the coordinate system, which were fit with a straight line with $-b$ as the slope. The fitting results when normal stress is 10 MPa is shown in Fig. 14, and b -values calculated from each sensor are 0.893, 0.831, 0.842 and 0.849, respectively. In addition to the b -value, the a -value can also be obtained from the fitting formulas, which reflects the total number of the AE hits during the shear process.

Changes in the average AE b -value with shear cycles under normal stresses of 1, 5, 7 and 10 MPa are shown in Fig. 15a, and the detailed b -values are listed in Table 4. b_1 , b_2 , b_3 and b_4 denote the b -values calculated by the AE data recorded by the first, second, third and fourth sensors, respectively (the Arabic numeral represents the label of the AE sensor). Nearly all of the b -values increase with shear cycles under a certain normal stress, indicating that the proportion of AE events with larger magnitude/amplitude gradually decreases with an increasing number of shear cycles. Based on Goebel et al. (2013) and Meng et al. (2016), a high b -value means that the stress concentration inside the fault plane is attenuated. Therefore, it can be deduced from the evolution of b -value with shear cycles that the energy accumulation and stress concentration in asperities gradually recede because of asperity damage and deterioration. This result is consistent with the analysis in Sect. 6.1 that energy cannot accumulate during subsequent shear cycles as it does in the first shear in the damaged asperities; thus, the earthquake and fault-slip rockburst disaster potential attributable to fault sliding is decreased.

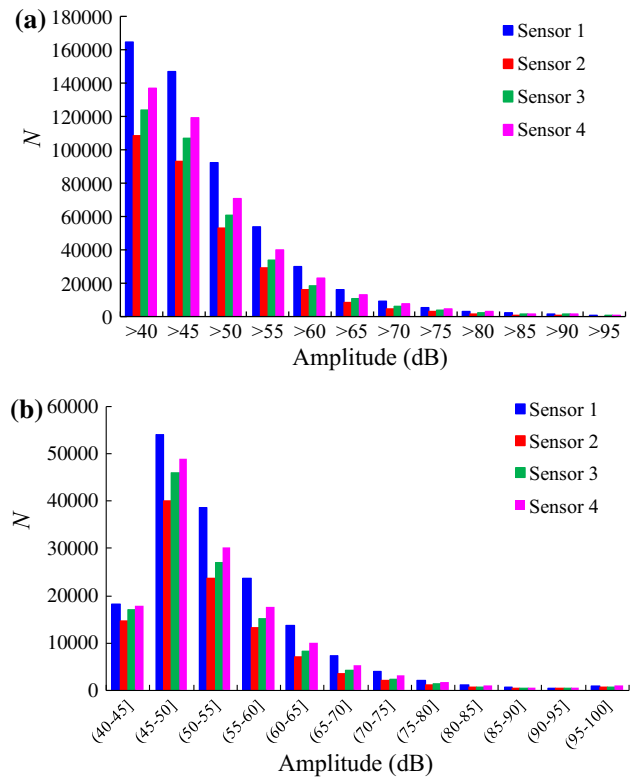


Fig. 13 Statistical relationship between AE amplitude and frequency when the normal stress was 10 MPa: the cumulative amplitude distribution (a) and the amplitude distribution (b)

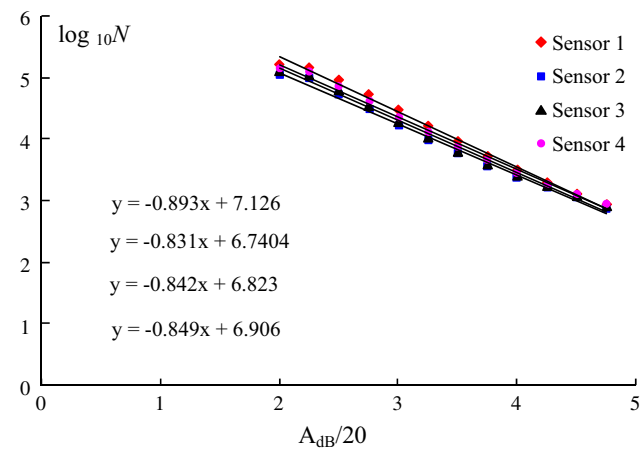


Fig. 14 Fitting result for the AE amplitude–frequency relationship at a normal load of 10 MPa; the formulas in the figure from top to bottom represent the results for sensors 1, 2, 3 and 4, respectively

Changes in the AE a -value (the intercept of the linear G–R law with the y-axis) are also given in Table 4, and Fig. 15b shows the average a -value with shear cycles under different normal stresses. The average a -value tends to decrease with an increasing number of shear cycles. This indicates that the total number of AE events decreases with shear cycles, which is consistent with the analysis in Sect. 5.2.

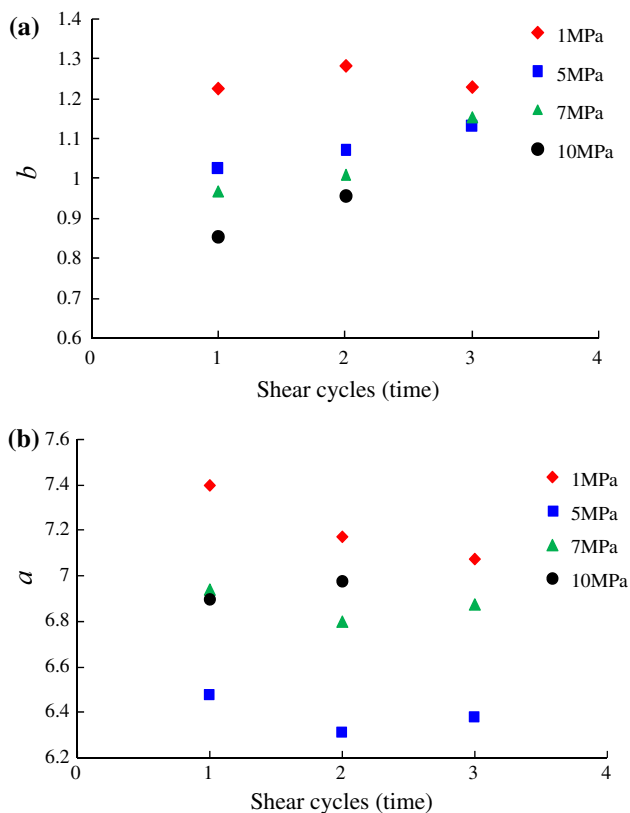


Fig. 15 Changes in the AE *b*- and *a*-values with shear cycles under different normal stresses

7 Discussion and Conclusions

This paper provides preliminary research results from shear tests of tensile granite joints, and some interesting phenomena are revealed and explained. However, some aspects require further study. For example, what promotes

stick–slip for granite joints? Is a planar or rough fresh joint favorable for stick–slip under the same normal stress? When stick–slip occurs, the shear stress initially increases, then decreases to a low value, increases again with shear displacement, and finally decreases abruptly to another low value. This process continues until the end of the test. Tensile cracks occur for granite joints under high normal stress, and there are far fewer cracks than the number of oscillations in the shear process; thus, the point at which the tensile cracks were generated cannot be determined from the tests. The factors that determine the frequency of stress oscillations (or the time interval between each stress drop) also require further investigation in a future study.

The 3D topography of the joint surface may greatly influence the shear behavior and AE distribution of one joint, but it is almost impossible to prepare several tensile joints with the same 3D topography. Therefore, when considering factors that affect the shear behavior of a tensile joint, such as normal stress or shear rate, the surface topography of each joint is not identical. Because of the limitations of experimental conditions, the 3D topography of the joint surface is not quantified, and only a rough comparison between the AE events distribution and surface asperity damage was conducted. Attempts were made to correlate the 2D roughness and the located AE events. Photographs taken before shear tests are used to draw the profile line from the side of specimen, as shown in Fig. 16, to reflect the two-dimensional roughness of the joint. The black solid line in Fig. 16a represents the expected split surface at the middle of the cubic specimen and also acts as the reference line of the profile, and the undulant blue line in Fig. 16b is the actual fracture surface after splitting. Correlation between the 2D roughness and the AE events is not obvious. The joint sheared under 10 MPa normal stress

Table 4 *b*- and *a*-value obtained from different sensors under various normal stresses

Normal stress (MPa)	Shear cycles	<i>b</i> 1	<i>a</i> 1	<i>b</i> 2	<i>a</i> 2	<i>b</i> 3	<i>a</i> 3	<i>b</i> 4	<i>a</i> 4	Average <i>b</i> -value	Average <i>a</i> -value
1	1	1.1718	7.2827	/	/	1.2902	7.4827	1.2191	7.4325	1.2270	7.3993
	2	1.2721	6.8864	/	/	1.2666	7.3087	1.3146	7.3229	1.2844	7.1727
	3	1.1941	6.6267	/	/	1.2491	7.4051	1.2432	7.1922	1.2288	7.0747
5	1	1.0771	6.4828	0.9702	6.4716	0.933	6.5704	0.9435	6.3836	0.98095	6.4771
	2	1.0667	6.2177	1.0718	6.4089	1.145	6.2642	1.2091	6.3618	1.1232	6.3131
	3	1.0916	6.2146	1.1701	6.5439	1.2115	6.4187	1.2319	6.3393	1.1763	6.3791
7	1	0.9794	7.0335	/	/	0.965	6.9616	0.9566	6.8223	0.9670	6.9391
	2	1.004	6.7226	/	/	1.0228	6.8953	0.9984	6.7727	1.0084	6.7969
	3	1.1506	6.777	/	/	1.1056	6.7526	1.2049	7.0895	1.1537	6.8730
10	1	0.8938	7.1265	0.8314	6.7404	0.8428	6.8232	0.8496	6.9064	0.8544	6.8991
	2	1.0034	7.3401	0.9385	6.8556	0.9511	6.9284	0.9295	6.7708	0.9556	6.9737

To improve the accuracy of the analysis results, the data were not used if the AE hits or energy recorded by one sensor deviated greatly from the others, such as data from the second sensor when normal stress is 1 and 7 MPa

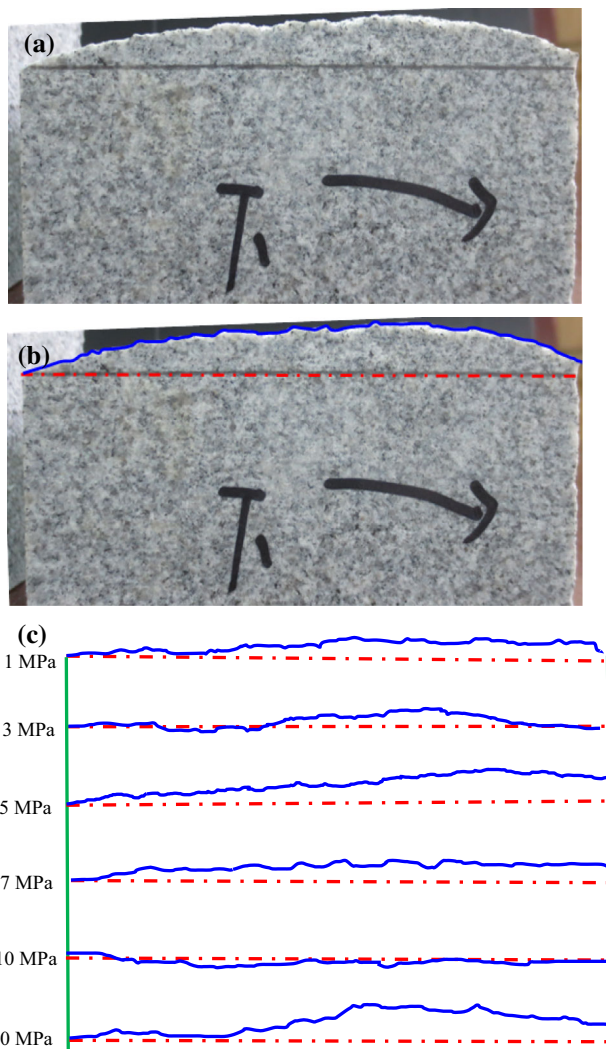


Fig. 16 Two-dimensional roughness profile of the joint under different normal stresses

has the lowest roughness, but density of AE events is higher than that of under lower normal stresses. The reason why it is difficult to establish relation between the number of AE events and 2D roughness can be summarized as follows. Firstly, the level of normal stress may be more important than the roughness of joint in generating AE events for the brittle and stiff granite, because more asperities are sheared off and more violent shear failure occurs under higher normal stress. Secondly, it is the 3D surface morphology that greatly affects the generation of AE events rather than the 2D roughness. The size and spatial distribution of the rough asperities on the joint surface determine the location and number of AE events. Besides, as anisotropy exists on the fracture surface roughness, shear behavior and AE activity are different when joint is sheared along different directions even with the same morphology. Accordingly, further studies are needed both to quantitatively evaluate the surface

characteristics before and after shear testing and to investigate the influence of the 3D morphology of joints on asperity damage by AE monitoring.

This study shows that AE monitoring is a useful and promising method for evaluating the asperity damage degree of rock joints. Compared to other methods, the AE technique can be used not only in laboratory studies but also for monitoring in situ jointed rock mass, and the real-time damage evolution process can be acquired based on the AE data. Additionally, the risk of dynamic hazard such as fault-slip rockburst can be estimated by analyzing the AE *b*-value.

Moment tensor analysis of AE events is also performed by some researchers to differentiate micro-tensile and shear cracks during rock failure under loading, and thus the failure mechanism can be analyzed. However, during shear failure of rock joint, the failure mechanism is much more complicated than just only shear or tensile failure mode, and AE signals come from the cracking, rolling, crushing, indentation, ploughing and sliding of asperities on the surface, and local fractures inside the intact rock; besides, the results analyzed by moment tensor method cannot be verified properly, and we do not know whether these results can reflect the real failure mechanism or not, because comparison cannot be easily made between the analysis result and the experimental results (the quantitative description of the failure modes in the shear test is nearly impossible, such as the number of shear crack or tensile crack, and only speculation can be made after shear tests based on the experimental phenomenon). So, the moment tensor method may be not the most satisfactory method to be used to investigate the micro-failure mechanism of rock joint, and more effort should be devoted to exploring this aspect.

The existence of joints makes the rock mass weaker, more deformable and highly anisotropic in strength. Hydraulic behavior is also greatly affected, and it is important to understand the mechanism of asperity degradation and the characteristics of asperity damage during the shearing process. In this study, shear tests were conducted on tensile granite joints under various normal stresses, and asperity damage was evaluated using the AE technique. The influences of asperity damage on joint shear behavior (such as dilation, stick-slip and the AE *b*-value) were also analyzed in detail. The following main conclusions can be drawn from this investigation:

- (a) The test results demonstrate that the AE technique is a good method for studying the asperity damage evolution in real time; the dilation curves can reflect the degradation of surface asperities and internal damage, such as the tensile fractures within the upper and lower intact rock.

- (b) Total AE events tend to increase with normal stress, and three stages can be determined in the cumulative event curve, the first turning point of which is defined as the *asperity damage initiation shear stress* (τ_{di}). Analysis indicates that τ_{di} is approximately 0.484 of τ_p and is unrelated to the normal stress level. Fewer than 10% of the total events are generated before τ_{di} , and 10–30 and 63–85% are radiated in the second and third stages, respectively, indicating that the majority of the damage occurs after the peak shear strength is reached.
- (c) Two stages (from compression to dilation) can be determined in the normal displacement curves when the normal stress is lower than 7 MPa, whereas three stages (compression, dilation and compression again) can be observed when the normal stress is higher than 20 MPa; the last compression may be caused by tensile failure that occurs outside the shear plane. Both the dilation and total AE events decrease with shear cycles because of the damage inflicted on asperities during the previous shear when the normal stress is lower than 10 MPa, and the normal displacement increases at a slower rate with shear displacement and remains nearly constant at the end of the shear because the damage to the asperities has reached the limit under the given level of normal stress.
- (d) The peaks on the shear stress graphs disappear when the joint is repeatedly sheared, and the ultimate shear strength in the first shear is nearly equal to the frictional strength in the second and third shear cycles. The magnitude of normal stress and the state of asperity are two important factors that control the post-peak stress drop and stick–slip of granite joints, and whether stress and energy are released in a slow or abrupt manner is dependent on the level of normal stress. Degradation of asperities during the first shear cycle will stop stick–slip from recurring in the second shear under the same normal stress because the ability to accumulate energy is decreased after serious deterioration of asperities.
- (e) The AE *b*-value increases with the number of shear cycles under different normal stresses, indicating that the stress concentration inside the fault plane attenuates as a result of asperity damage, and the dynamic disasters caused by unstable slip of the fault plane, such as the fault-slip rockburst, decrease. With an increasing number of shear cycles, the average AE *a*-value tends to decrease, meaning that the total number of AE events decreases, which is consistent with the analysis of AE events with shear cycles.

Acknowledgements We gratefully acknowledge financial support from the National Program on Key Basic Research Project of China under Grant No. 2014CB046902 and the National Science Foundation of China under Grant Nos. 41172288, 41472270, 41372298 and 51609121. The work in this paper was also supported by the Natural Science Foundation of Shandong Province (Grant No. ZR2016EEQ22), the China Postdoctoral Science Foundation (2016M602109) and the Open Research Fund of State Key Laboratory of Geomechanics and Geotechnical Engineering, Institute of Rock and Soil Mechanics, Chinese Academy of Sciences (Grant No. Z015007).

References

- Ai C, Zhang J, Li YW et al (2016) Estimation criteria for rock brittleness based on energy analysis during the rupturing process. *Rock Mech Rock Eng* 49(12):4681–4698. doi:10.1007/s00603-016-1078-x
- Asadi MS, Rasouli V, Barla G (2012) A bonded particle model simulation of shear strength and asperity degradation for rough rock fractures. *Rock Mech Rock Eng* 45:649–675. doi:10.1007/s00603-012-0231-4
- Asadi MS, Rasouli V, Barla G (2013) A Laboratory shear cell used for simulation of shear strength and asperity degradation of rough rock fractures. *Rock Mech Rock Eng* 46:683–699. doi:10.1007/s00603-012-0322-2
- Bahaaddini M, Sharrock G, Hebblewhite BK (2013) Numerical direct shear tests to model the shear behaviour of rock joints. *Comput Geotech* 51:101–115. doi:10.1016/j.comgeo.2013.02.003
- Bahaaddini M, Hagan PC, Mitra R, Khosravi MH (2016) Experimental and numerical study of asperity degradation in the direct shear test. *Eng Geol* 204:41–52. doi:10.1016/j.enggeo.2016.01.018
- Brace WF, Byerlee JD (1966) Stick–slip as a mechanism for earthquakes. *Science* 153:990–992. doi:10.1126/science.153.3739.990
- Chan CH, Wu YM, Tseng TL, Lin T, Chen C (2012) Spatial and temporal evolution of *b*-values before large earthquakes in Taiwan. *Tectonophysics* 532–535:215–222. doi:10.1016/j.tecto.2012.02.004
- Cho N, Martin CD, Sego DC (2008) Development of a shear zone in brittle rock subjected to direct shear. *Int J Rock Mech Min Sci* 45:1335–1346. doi:10.1016/j.ijrmms.2008.01.019
- Colombo IS, Main IG, Forde MC (2003) Assessing damage of reinforced concrete beam using “*b*-value” analysis of acoustic emission signal. *J Mater Civ Eng* 15:280–286. doi:10.1061/(ASCE)0899-1561(2003)15:3(280)
- Goebel THW, Schorlemmer D, Becker TW, Dresen G, Sammis CG (2013) Acoustic emissions document stress changes over many seismic cycles in stick–slip experiments. *Geophys Res Lett* 40:2049–2054. doi:10.1002/grl.50507
- Grasselli G (2001) Shear strength of rock joints based on quantified surface description. Ph.D. Thesis, Swiss Federal Institute of Technology (EPFL), Lausanne, Switzerland
- Grasselli G, Egger P (2003) Constitutive law for the shear strength of rock joints based on three-dimensional surface parameters. *Int J Rock Mech Min Sci* 40:25–40. doi:10.1016/S1365-1609(02)00101-6
- Grasselli G, Wirth J, Egger P (2002) Quantitative three-dimensional description of a rough surface and parameter evolution with shearing. *Int J Rock Mech Min Sci* 39:789–800. doi:10.1016/S1365-1609(02)00070-9
- Gutenberg B, Richter CF (1944) Frequency of earthquakes in California. *Bull Seismol Soc Am* 34:185–188

- Hong E, Kwon T, Song K, Cho G (2016) Observation of the degradation characteristics and scale of unevenness on three-dimensional artificial rock joint surfaces subjected to shear. *Rock Mech Rock Eng* 49:3–17. doi:[10.1007/s00603-015-0725-y](https://doi.org/10.1007/s00603-015-0725-y)
- Huang X, Haimson BC, Plesha ME, Qiu X (1993) An investigation of the mechanics of rock joints—part I. Laboratory investigation. *Int J Rock Mech Min Sci Geomech Abstr* 30:257–269. doi:[10.1016/0148-9062\(93\)92729-A](https://doi.org/10.1016/0148-9062(93)92729-A)
- Hutson RW, Dowding CH (1990) Joint asperity degradation during cyclic shear. *Int J Rock Mech Min Sci Geomech Abstr* 27:109–119. doi:[10.1016/0148-9062\(90\)94859-R](https://doi.org/10.1016/0148-9062(90)94859-R)
- Indraratna B, Thirukumaran S, Brown ET, Premadasa W, Gale W (2014) A technique for three-dimensional characterisation of asperity deformation on the surface of sheared rock joints. *Int J Rock Mech Min Sci* 70:483–495. doi:[10.1016/j.ijrmmms.2014.04.022](https://doi.org/10.1016/j.ijrmmms.2014.04.022)
- Indraratna B, Thirukumaran S, Brown ET, Zhu S (2015) Modelling the shear behaviour of rock joints with asperity damage under constant normal stiffness. *Rock Mech Rock Eng* 48:179–195. doi:[10.1007/s00603-014-0556-2](https://doi.org/10.1007/s00603-014-0556-2)
- Jafari MK, Hosseini KA, Pellet F, Boulon M, Buzzi O (2003) Evaluation of shear strength of rock joints subjected to cyclic loading. *Soil Dyn Earthq Eng* 23:619–630. doi:[10.1016/S0267-7261\(03\)00063-0](https://doi.org/10.1016/S0267-7261(03)00063-0)
- Karami A, Stead D (2008) Asperity degradation and damage in the direct shear test: a hybrid FEM/DEM approach. *Rock Mech Rock Eng* 41:229–266. doi:[10.1007/s00603-007-0139-6](https://doi.org/10.1007/s00603-007-0139-6)
- Khosravi A (2016) Estimation and validation of post-peak behavior of hard rocks. Ph.D. Dissertation, Ecole Polytechnique Montreal, Montreal
- Lee HS, Park YJ, Cho TF, You KH (2001) Influence of asperity degradation on the mechanical behavior of rough rock joints under cyclic shear loading. *Int J Rock Mech Min Sci* 38:967–980. doi:[10.1016/S1365-1609\(01\)00060-0](https://doi.org/10.1016/S1365-1609(01)00060-0)
- Li K, Cao P, Zhang K, Zhong Y (2015) Macro and meso characteristics evolution on shear behavior of rock joints. *J Cent South Univ* 22:3087–3096. doi:[10.1007/s11771-015-2845-7](https://doi.org/10.1007/s11771-015-2845-7)
- Meng FZ, Zhou H, Zhang CQ et al (2015) Evaluation methodology of brittleness of rock based on post-peak stress–strain curves. *Rock Mech Rock Eng* 48(5):1787–1805. doi:[10.1007/s00603-014-0694-6](https://doi.org/10.1007/s00603-014-0694-6)
- Meng FZ, Zhou H, Wang ZQ, Zhang L, Kong L, Li S, Zhang C (2016) Experimental study on the prediction of rockburst hazards induced by dynamic structural plane shearing in deeply buried hard rock tunnels. *Int J Rock Mech Min Sci* 86:210–223. doi:[10.1016/j.ijrmmms.2016.04.013](https://doi.org/10.1016/j.ijrmmms.2016.04.013)
- Moradian ZA, Ballivy G, Rivard P, Gravel C, Rousseau B (2010) Evaluating damage during shear tests of rock joints using acoustic emissions. *Int J Rock Mech Min Sci* 47:590–598. doi:[10.1016/j.ijrmmms.2010.01.004](https://doi.org/10.1016/j.ijrmmms.2010.01.004)
- Moradian ZA, Ballivy G, Rivard P (2012) Correlating acoustic emission sources with damaged zones during direct shear test of rock joints. *Can Geotech J* 49:710–718. doi:[10.1139/t2012-029](https://doi.org/10.1139/t2012-029)
- Nanjo KZ, Hirata N, Obara K, Kasahara K (2012) Decade-scale decrease in b value prior to the M 9-class 2011 Tohoku and 2004 Sumatra quakes. *Geophys Res Lett* 39:L20304. doi:[10.1029/2012GL052997](https://doi.org/10.1029/2012GL052997)
- Nejati HR, Ghazvinian A (2014) Brittleness effect on rock fatigue damage evolution. *Rock Mech Rock Eng* 47:1839–1848. doi:[10.1007/s00603-013-0486-4](https://doi.org/10.1007/s00603-013-0486-4)
- Nuannin P, Kulhánek O, Persson L (2012) Variations of b-values preceding large earthquakes in the Andaman–Sumatra subduction zone. *J Asian Earth Sci* 61:237–242. doi:[10.1016/j.jseae.2012.10.013](https://doi.org/10.1016/j.jseae.2012.10.013)
- Park J, Song J (2009) Numerical simulation of a direct shear test on a rock joint using a bonded-particle model. *Int J Rock Mech Min Sci* 46:1315–1328. doi:[10.1016/j.ijrmmms.2009.03.007](https://doi.org/10.1016/j.ijrmmms.2009.03.007)
- Pereira JP, de Freitas MH (1993) Mechanisms of shear failure in artificial fractures of sandstone and their implication for models of hydromechanical coupling. *Rock Mech Rock Eng* 26:195–214. doi:[10.1007/BF01040115](https://doi.org/10.1007/BF01040115)
- Plesha ME (1987) Constitutive models for rock discontinuities with dilatancy and surface degradation. *Int J Numer Anal Methods Geomech* 11:345–362. doi:[10.1002/nag.1610110404](https://doi.org/10.1002/nag.1610110404)
- Qiu X, Plesha ME, Huang X, Haimson BC (1993) An investigation of the mechanics of rock joints. Part II—analytical investigation. *Int J Rock Mech Min Sci Geomech Abstr* 30:271–287. doi:[10.1016/0148-9062\(93\)92730-E](https://doi.org/10.1016/0148-9062(93)92730-E)
- Rao M, Lakshmi KJP (2005) Analysis of b-value and improved b-value of acoustic emissions accompanying rock. *Curr Sci* 89:1577–1582
- Sainoki A, Mitri HS (2014a) Dynamic modelling of fault slip with Barton's shear strength model. *Int J Rock Mech Min Sci* 67:155–163
- Sainoki A, Mitri HS (2014b) Simulating intense shock pulses due to asperities during fault-slip. *J Appl Geophys* 103:71–81. doi:[10.1016/j.jappgeo.2014.01.009](https://doi.org/10.1016/j.jappgeo.2014.01.009)
- Sainoki A, Mitri HS (2015) Evaluation of fault-slip potential due to shearing of fault asperities. *Can Geotech J* 52:1417–1425
- Scholz CH (1968) The frequency–magnitude relation of microfracturing in rock and its relation to earthquakes. *Bull Seismol Soc Am* 58:399–415
- Schorlemmer D, Wiemer S (2005) Earth science: microseismicity data forecast rupture area. *Nature* 434:1086. doi:[10.1038/4341086a](https://doi.org/10.1038/4341086a)
- Singh HK, Basu A (2016) Shear behaviors of ‘real’ natural un-matching joints of granite with equivalent joint roughness coefficients. *Eng Geol* 211:120–134. doi:[10.1016/j.enggeo.2016.07.004](https://doi.org/10.1016/j.enggeo.2016.07.004)
- Smith WD (1981) The b-value as an earthquake precursor. *Nature* 289:136–139. doi:[10.1038/289136a0](https://doi.org/10.1038/289136a0)
- Tang ZC, Wong LNY (2016) New criterion for evaluating the peak shear strength of rock joints under different contact states. *Rock Mech Rock Eng* 49:1191–1199. doi:[10.1007/s00603-015-0811-1](https://doi.org/10.1007/s00603-015-0811-1)
- Tarasov BG (2014) Fan-structure shear rupture mechanism as a source of shear rupture rockbursts. *J South Afr Inst Min Metall* 114:773–784
- Tarasov BG, Randolph MF (2011) Super brittleness of rocks and earthquake activity. *Int J Rock Mech Min Sci* 48(6):888–898. doi:[10.1016/j.ijrmmms.2011.06.013](https://doi.org/10.1016/j.ijrmmms.2011.06.013)
- Wang W, Scholz CH (1994) Wear processes during frictional sliding of rock: a theoretical and experimental study. *J Geophys Res* 99:6789–6799. doi:[10.1029/93JB02875](https://doi.org/10.1029/93JB02875)
- Wang J, Chen K, Leu P, Chang C (2016) Precursor times of abnormal b-values prior to mainshocks. *J Seismol* 20:905–919. doi:[10.1007/s10950-016-9567-7](https://doi.org/10.1007/s10950-016-9567-7)
- Wawersik WR, Brace WF (1971) Post-failure behavior of a granite and diabase. *Rock Mech* 3:61–85
- Zou DH (1988) Numerical analysis of rock failure and laboratory study of the related acoustic emission. Ph.D. Thesis, University British Columbia, Vancouver
- Zou D, Miller HDS, Kaiser PK (1989) Numerical study of violent rock failure by stick-slip on joints. *Min Sci Technol* 9:241–251. doi:[10.1016/S0167-9031\(89\)90958-4](https://doi.org/10.1016/S0167-9031(89)90958-4)